

Imaging of Sources in Heavy-Ion Reactions

David A. Brown* and Paweł Danielewicz†

*National Superconducting Cyclotron Laboratory and
Department of Physics and Astronomy, Michigan State University,
East Lansing, Michigan 48824, USA*

(August 7, 2018)

Abstract

Imaging of sources from data within the intensity interferometry is discussed. In the two-pion case, the relative pion source function may be determined by Fourier transforming the correlation function. In the proton-proton case, the discretized source function may be fitted to the correlation data.
PACS numbers: 25.75.Gz, 25.75.-q

Typeset using REVTeX

*e-mail: dbrown@nscl.msu.edu

†e-mail: danielewicz@nscl.msu.edu

Phase interferometry [1] is capable of delivering star images in astronomy, e.g. that of Betelgeuse [2]. Intensity interferometry, as is applied in nuclear physics, has primarily been used to determine radii of stars in astronomy and of particle emitting regions in heavy-ion reactions. In heavy-ion reactions, this determination has most often been done by fitting the low-momentum two-particle correlation functions under the assumption of Gaussian-shaped emitting regions [3]. Similarly, source lifetimes have been inferred by considering Gaussian-shaped distributions of emission times. However, it was not always clear that the analyzed data truly narrows down the lifetime for short-lived sources. Bertsch [4] and Mrówczyński [5] noted that an integral over the low-momentum correlation function can yield the value of the source function at the zero relative distance. Beyond this, no attempts were made to image the source function from the reaction data. Typically, comparison to reaction simulations is carried out by generating the correlation functions from simulated events.

In this letter, we investigate the feasibility of direct imaging of the source from reaction data, within the intensity interferometry. Given a two-particle correlation function, this represents an inversion problem. We consider two examples: that of like-charged-pion and that of proton-proton interferometry. In the like-pion case, the relative source function is a Fourier transformation of the two-particle correlation function. In the proton case, the procedure is more involved. In this letter, we first discuss the relation of the correlation function to the source function, then the imaging, and finally some information contained in the images.

Under the assumption of the approximate independence of processes leading to two particles in the final state and the assumption of the weak dependence of the product of single-particle sources \overline{D} on momenta important for correlations, the two-particle correlation function may be represented as [6,7]

$$C_{\mathbf{P}}(\mathbf{q}) = \frac{dN_2/d\mathbf{p}_1 d\mathbf{p}_2}{(dN_1/d\mathbf{p}_1)(dN_1/d\mathbf{p}_2)} \simeq \int d\mathbf{r} |\Phi_{\mathbf{q}}^{(-)}(\mathbf{r})|^2 S_{\mathbf{P}}(\mathbf{r}). \quad (1)$$

Here $S_{\mathbf{P}}(\mathbf{r})$ is the distribution of relative separation of emission points for the two particles, in their center of mass. In terms of single-particle sources,

$$S_{\mathbf{P}}(\mathbf{r}) = \int d\mathbf{R} dt_1 dt_2 \overline{D}(0, \mathbf{R} + \mathbf{r}/2, t_1) \overline{D}(0, \mathbf{R} - \mathbf{r}/2, t_2). \quad (2)$$

The momentum \mathbf{P} above is the total momentum of the pair and \mathbf{q} is the cm relative momentum. The integrations in (1) and in (2) are over cm variables; the single-particles sources, $\overline{D} = D / \int d\mathbf{r} dt D$, are taken in the pair cm frame. The function D is the distribution of last collisions for an emitted particle in space, time, and momentum. Both S and \overline{D} are normalized to 1. For Klein-Gordon fields, with $(\square + m_\pi^2)\phi(x) = -j(x)$, D may be written in terms of single-particle self-energies as

$$D(\mathbf{p}, \mathbf{r}, t) = \frac{i}{2E_p} \Pi^<(\mathbf{p}, E_p, \mathbf{r}, t) \exp \left[-\frac{1}{2E_p} \int_t^\infty dt' (-2)\text{Im} \Pi^+(\mathbf{p}, E_p, \mathbf{r} + \mathbf{v}_p(t' - t), t') \right], \quad (3)$$

where $i\Pi^<(x, x') = \langle j(x') j(x) \rangle_{\text{irred}}$, and $(-2)\text{Im} \Pi^+(x, x') = \langle [j(x), j(x')] \rangle_{\text{irred}}$. For the Schrödinger fields, with $(i\frac{\partial}{\partial t} + \frac{\nabla^2}{2m})\Psi(x) = j(x)$, the analogous result is

$$D(\mathbf{p}, \mathbf{r}, t) = \mp i\Sigma^<(\mathbf{p}, E_p, \mathbf{r}, t) \exp \left[-\int_t^\infty dt' \Gamma(\mathbf{p}, E_p, \mathbf{r} + \mathbf{v}_p(t' - t), t') \right], \quad (4)$$

where $\mp i\Sigma^<$ is the single-particle production rate, $\mp i\Sigma^<(x, x') = \langle j(x') j(x) \rangle_{\text{irred}}$, and Γ is the damping rate. For particles with spin, the modulus of the wavefunction in (1) should be averaged over spin directions. For low r within the source, deviations from (2) could be expected in the presence of short-range repulsion. Results (1), (3), and (4) ignore the final-state refraction. We discuss the effects of the Coulomb field of a source in a separate paper [8]. For pion-pion correlations, both these effects and the effects of the pion-pion Coulomb interaction may be approximately removed directly from the correlation function [9].

While the correlation function C has an *indirect* dependence on other quantities, it is shaped directly by S in the reaction, i.e. by the relative distribution of emission points for two particles with similar momenta, in their center of mass. For like particles, S is a symmetric function. This is not generally the case for distinct particles. Depending on the circumstances in a reaction, S may range from isotropic, for prompt emission, to strongly elongated along \mathbf{P} , and possibly even bone-shaped, for emission from a long-lived source. In

this last case, the transverse size would be close to the size of a nucleus at short distances along \mathbf{P} and widen at larger distances due to the zigzagging of the source under the recoil caused by emission. The lifetime might be read off from the elongation of S .

With (1), the goal of the imaging is the determination of S given C . Given that the interesting part of C is its deviation from 1, we may subtract 1 from both sides of (1) obtaining

$$C_{\mathbf{P}}(\mathbf{q}) - 1 = \int d\mathbf{r} \left(|\Phi_{\mathbf{q}}^{(-)}(\mathbf{r})|^2 - 1 \right) S_{\mathbf{P}}(\mathbf{r}) = \int d\mathbf{r} K(\mathbf{q}, \mathbf{r}) S_{\mathbf{P}}(\mathbf{r}), \quad (5)$$

where $K = |\Phi_{\mathbf{q}}^{(-)}|^2 - 1$. The problem of imaging then reduces to the inversion of K . A difficulty may arise from the presence of a kernel (or null-space) of K , i.e. the subspace of functions that the operator K turns to zero. The projection of S onto the kernel cannot be restored within imaging. It will become apparent that, in the case of like particles, the kernel of K is empty. For unlike particles, when one of the particles is neutral, the imaging may not be able to restore portions of S for large particle separations as K approaches zero for large separations; a particular severe situation occurs for $|\Phi_{\mathbf{q}}^{(-)}|^2 \simeq 1$, when the whole space of functions becomes the kernel.

For like-pion pairs, Eq. (5) may be written as

$$C_{\mathbf{P}}(\mathbf{q}) - 1 = \int d\mathbf{r} \cos(2\mathbf{q} \cdot \mathbf{r}) S_{\mathbf{P}}(\mathbf{r}), \quad (6)$$

if we ignore interactions between the pions. Given that S is symmetric, the Fourier transform can be inverted to yield

$$S_{\mathbf{P}}(\mathbf{r}) = \frac{1}{\pi^3} \int d\mathbf{q} \cos(2\mathbf{q} \cdot \mathbf{r}) (C_{\mathbf{P}}(\mathbf{q}) - 1). \quad (7)$$

The directions that we use in the analysis of S are, in the system frame, outward along the transverse momentum of the pair, longitudinal along the beam, and the remaining direction, termed transverse. With equation (7), we can find the angular moments of the source and the correlation function. If we introduce $C(\mathbf{q}) = \sqrt{4\pi} \sum_{\lambda m} C^{\lambda m}(q) Y^{\lambda m}(\Omega_{\mathbf{q}})$ and an analogous representation for S , then we get the relation

$$S_{\mathbf{P}}^{\lambda m}(r) = \frac{(-1)^{\lambda/2} 4}{\pi^2} \int_0^\infty dq q^2 j_\lambda(2qr) (C_{\mathbf{P}}^{\lambda m}(r) - \delta^{\lambda 0} \delta^{m 0}). \quad (8)$$

Due to the symmetry of S and C , only even λ appear in the angular expansion of these functions. Since both functions are real, the moments satisfy $(C^{\lambda m})^* = (-1)^m C^{\lambda - m}$. The relation (8) between the angular moments may help in analyzing the three-dimensional data. In particular, this relation shows that the angle-averaged correlation function $C^{00}(q) \equiv C(q)$ reflects the angle-averaged source $S^{00}(r) \equiv S(r)$,

$$r S_{\mathbf{P}}(r) = \frac{2}{\pi^2} \int_0^\infty dq q \sin(2qr) (C_{\mathbf{P}}(q) - 1). \quad (9)$$

As a specific example of the source extraction, in Fig. 1 we present the relative angle-averaged π^- source-function. It is determined by applying Eq. (9) to the data of Ref. [10] for central 10.8 GeV/c Au + Au. Prior to the Fourier transformation in (9), the data were corrected for the Coulomb interaction between the two pions and between the pions and the source [9]. The integration in (9) for Fig. 1 was cut off at $q_{\max} \simeq 50$ MeV/c, giving a resolution in the relative distance in the figure of $\Delta r \sim 1/2q_{\max} \sim 2.0$ fm. The largest r that may be considered is $1/2 \Delta q$, where Δq is the momentum resolution of the data ($\Delta q = 5$ MeV/c in the case of [10]).

In the general case, the respective angular moments of C and S are also directly related. The spin-averaged operator, K , only depends on the angle between \mathbf{q} and \mathbf{r} , and not on their separate directions. Thus, the averaged K may be expanded: $K(\mathbf{q}, \mathbf{r}) = \sum_\lambda (2\lambda + 1) K_\lambda(q, r) P^\lambda(\cos \theta)$. A relation between the moments follows from (5),

$$C_{\mathbf{P}}^{\lambda m}(q) - \delta^{\lambda 0} \delta^{m 0} = 4\pi \int_0^\infty dr r^2 K_\lambda(q, r) S_{\mathbf{P}}^{\lambda m}(r). \quad (10)$$

In the like-nucleon and like-charged-pion cases, the $\lambda = 0$ operator is

$$K_0(q, r) = \frac{1}{2} \sum_{js\ell\ell'} (2j + 1) \left(g_{js}^{\ell\ell'}(r) \right)^2 - 1, \quad (11)$$

where $g_{js}^{\ell\ell'}$ is the radial wave function with outgoing asymptotic angular momentum ℓ . If the correlations are of purely Coulomb origin, such as between intermediate-mass fragments [11], the operator is $K_0(q, r) = \theta(r - r_c) (1 - r_c/r)^{1/2} - 1$ in the classical limit. Here r_c is the distance of closest approach, $r_c(q) = 2\mu Z_1 Z_2 e^2/q^2$.

We determine the source by discretizing the functions and integrals in equations such as (1), (5), or (10), and fitting the discretized values of S . We illustrate this by analyzing the proton-proton correlation data [12,13] from the 75 MeV/nucleon $^{14}\text{N} + ^{27}\text{Al}$ reaction, displayed in Fig. 2.

With the data [13] averaged over the \mathbf{q} directions, we concentrate on the relation (10) between the angle-averaged S and C . At high relative-momenta, the assumptions leading to (1) may break down. Further, at high momentum correlations within the source, such as associated with the anisotropic flow [14], may play a role. In addition, the event selection for singles in [13] becomes an issue. Thus we restrict the region for source determination to less than $q_{\max} \simeq 80$ MeV/c. Given the issues of experimental resolution [13], we restrict the region of analysis from below to $q > q_{\min} = 10$ MeV/c. This sets a lower limit on the resolution within the source of $1/2(q_{\max} - q_{\min}) \simeq 1.4$ fm. Therefore, we settle with a determination of the source values at points separated by a coarser $\Delta r = 1.8$ fm. We represent the source function as

$$S_{\mathbf{P}}(r) \simeq \sum_k S_{\mathbf{P}}(r_k) g(r - r_k), \quad (12)$$

where $r_k = (k - \frac{1}{2})\Delta r$ and g is a profile function, $g(x) = 1$ for $|x| < \Delta r/2$, and $g(x) = 0$ otherwise. Then from (10), we get

$$C_{\mathbf{P}}(q) - 1 \simeq \sum_k w_k(q) S_{\mathbf{P}}(r_k), \quad (13)$$

where $w_k = 4\pi \int dr r^2 K_0(q, r) g(r - r_k)$. We determine the pp wavefunctions for $\ell, \ell' \leq 2$ from the Schrödinger equation with the regularized Reid soft-core potential [15]. Finally we minimize $\chi_{\mathbf{P}}^2 = \sum_j ((C_{\mathbf{P}}^{\text{exp}}(q_j) - C_{\mathbf{P}}(q_j))/\sigma_j)^2$ by varying $S(r_k)$, subject to the conditions that $S(r_k) \geq 0$ and that S is normalized to 1. Initially, we aimed to determine the source up to $r_{\max} \sim 30$ fm, but we found that the fits favored S consistent with zero at higher r . Thus, we were able to reduce r_{\max} to 16.2 fm without an appreciable worsening in the fits.

The source functions extracted from the data [12,13] are shown for the three total-momentum gates in Fig. 3 together with the source functions determined directly within

Boltzmann-equation reaction-simulations [16,12]. Unlike what was done in [12], we initialize the nuclear matter density in the model by solving the Thomas-Fermi equations. The errors on the extracted S include the uncertainty from varying q_{\max} in the vicinity of 80 MeV/c. The values of χ^2 per degree of freedom are 1.1 for the highest momentum gate, 1.8 for the lowest, and 4.9 for the intermediate one with the lowest errors on the data.

We now discuss the relative proton source functions extracted from the data and calculated in the model, together with the information contained in source functions. The change in the relative distribution of emission points in Fig. 3, from a compact form at high proton momenta to an extended form at low momenta, demonstrate the presence of space-momentum correlations within the $^{14}\text{N} + ^{27}\text{Al}$ reaction. At intermediate and low momenta, neither the relative proton distributions from the data, nor those from the model, can be well approximated by Gaussians. This is in contrast to the distribution in Fig. 1, and to a degree, to distributions for high momenta in Fig. 3. Overall, the transport model yields distributions in a near-quantitative agreement with the experimental sources. The model source seems to systematically underestimate the values from the data only at the shortest r .

For a rapid freeze-out, the single-particle source is given by $D(\mathbf{p}, \mathbf{r}, t) \simeq f(\mathbf{p}, \mathbf{r}) \delta(t - t_0)$ where f is the Wigner function. Assuming weak *directional* correlations between the pair total and relative momenta, and between the spatial and momentum variables, the momentum average of S approximates the relative distribution of emission points for any two particles from the reaction, and not just for the particles with close momenta. Thus given a rapid freeze-out, the relative distribution for any two particles is

$$\mathcal{S}(\mathbf{r}) = \frac{\int d\mathbf{P} d\mathbf{p} d\mathbf{R} f(\mathbf{P}/2 + \mathbf{p}, \mathbf{R} + \mathbf{r}/2) f(\mathbf{P}/2 - \mathbf{p}, \mathbf{R} - \mathbf{r}/2)}{\int d\mathbf{p}_1 d\mathbf{r}_1 f(\mathbf{p}_1, \mathbf{r}_1) \int d\mathbf{p}_2 d\mathbf{r}_2 f(\mathbf{p}_2, \mathbf{r}_2)}. \quad (14)$$

We now rewrite and expand the expression in the numerator in (14):

$$\begin{aligned} & f(\mathbf{P}/2 + \mathbf{p}, \mathbf{R} + \mathbf{r}/2) f(\mathbf{P}/2 - \mathbf{p}, \mathbf{R} - \mathbf{r}/2) \\ &= \int d\mathbf{r}'_1 f(\mathbf{p}_1, \mathbf{r}'_1) \int d\mathbf{r}'_2 f(\mathbf{p}_2, \mathbf{r}'_2) \frac{f(\mathbf{P}/2 + \mathbf{p}, \mathbf{R} + \mathbf{r}/2) f(\mathbf{P}/2 - \mathbf{p}, \mathbf{R} - \mathbf{r}/2)}{\int d\mathbf{r}'_1 f(\mathbf{p}_1, \mathbf{r}'_1) \int d\mathbf{r}'_2 f(\mathbf{p}_2, \mathbf{r}'_2)} \\ &= \int d\mathbf{r}'_1 f(\mathbf{p}_1, \mathbf{r}'_1) \int d\mathbf{r}'_2 f(\mathbf{p}_2, \mathbf{r}'_2) \left(1 + \mathbf{p} \frac{\partial}{\partial \mathbf{p}'} + \dots \right) \end{aligned}$$

$$\times \frac{f(\mathbf{P}/2 + \mathbf{p}', \mathbf{R} + \mathbf{r}/2) f(\mathbf{P}/2 - \mathbf{p}', \mathbf{R} - \mathbf{r}/2)}{\int d\mathbf{r}'_1 f(\mathbf{P}/2 + \mathbf{p}', \mathbf{r}'_1) \int d\mathbf{r}'_2 f(\mathbf{P}/2 - \mathbf{p}', \mathbf{r}'_2)} \Big|_{\mathbf{p}'=0}. \quad (15)$$

The gradient term must be proportional to a combination of the vectors \mathbf{P} , \mathbf{r}_1 , and \mathbf{r}_2 . For weak directional correlations, it then averages to zero under the integration in (14). Inserting (15) into (14) and keeping the leading term, we obtain

$$\mathcal{S}(\mathbf{r}) \simeq \frac{1}{N^2} \int d\mathbf{p}_1 d\mathbf{p}_2 \frac{dN}{d\mathbf{p}_1} \frac{dN}{d\mathbf{p}_2} \gamma_P S_{\mathbf{P}}(\mathbf{r} + \mathbf{n}_{\mathbf{P}} (\gamma_P - 1)(\mathbf{n}_{\mathbf{P}} \mathbf{r})), \quad (16)$$

where N is particle multiplicity and $\mathbf{n}_{\mathbf{P}} = \mathbf{P}/P$. The argument of $S_{\mathbf{P}}$ has been written in the cm frame of an emitted pair and γ_P is the Lorentz factor for the transformation from the system frame to the pair cm frame.

Generally the relative distribution of emission points for any two particles at $r \rightarrow 0$ gives an average freeze-out density when multiplied by $N - 1$. If the assumptions above are valid, this density may be obtained by multiplying the average (16) of $S_{\mathbf{P}}(r \rightarrow 0)$ by $N - 1$. The transport calculations [16] indicate that the measured [13] coincidence cross sections for the $^{14}\text{N} + ^{27}\text{Al}$ reaction are dominated by rather central collisions with $b \sim 2.8$ fm. The chance of detecting two particles at wide angles simultaneously is large only for these collisions. The rms nucleon cm momentum in central collisions is ~ 185 MeV/c and at 25° this corresponds to a lab momentum of ~ 320 MeV/c for the nucleon or ~ 640 MeV/c total for the pair. Thus, the results for the intermediate-momentum gate in Fig. 3 best represent the average situation in the central collision. Presuming that the relative spatial distributions of other particles to protons is similar to that of two protons, we arrive at an average nuclear density in the vicinity of any emitted proton of $17 \times S(r \rightarrow 0) \simeq 17 \times 0.0015 \text{ fm}^{-3} = 0.025 \text{ fm}^{-3} = 0.16 n_0$. Here we assume the participants to have a total mass of 18 following from the fireball geometry at $b \approx 2.8$ fm. The directional space-momentum correlations anticipated in collisions due to a collective motion, to shadowing, or to emission that is most likely not instantaneous, make this value an upper limit on the freeze-out density.

Irrespective of any correlations or of the validity of instantaneous freeze-out, the product

of the $r \rightarrow 0$ source-function and the momentum distribution yields the space average of the phase-space occupancy at freeze-out,

$$\langle f(\mathbf{p}) \rangle = \frac{(2\pi)^3}{2s+1} \frac{E_p}{m} \frac{dN}{d\mathbf{p}} S_{2\mathbf{p}}(r \rightarrow 0), \quad (17)$$

(see also [4]). Refs. [13,12] only give the inclusive proton cross-sections in the $^{14}\text{N} + ^{27}\text{Al}$ reaction at two angles. Furthermore, the cross sections include large contributions from peripheral events. Under these circumstances, we instead use the thermal distribution $dN_{\text{th}}/d\mathbf{p} \propto 1/(z^{-1} e^{p^2/2mT} + 1)$ for the central events in formula (17). Here, z is set from the requirement of maximum entropy. For ~ 9 participant protons at $b = 2.8$ fm in the $^{14}\text{N} + ^{27}\text{Al}$ reaction, this requirement gives $z \sim 1.10$ and $T \approx 10.2$ MeV. Equation (17) can now be used to determine the phase-space average of the occupancy at freeze-out, $\langle f \rangle = \int d\mathbf{p} (\langle f(\mathbf{p}) \rangle)^2 / \int d\mathbf{p} \langle f(\mathbf{p}) \rangle$, and to estimate the entropy per nucleon,

$$\frac{S}{A} \approx - \frac{\int d\mathbf{p} (\langle f(\mathbf{p}) \rangle \log (\langle f(\mathbf{p}) \rangle) - (1 - \langle f(\mathbf{p}) \rangle) \log (1 - \langle f(\mathbf{p}) \rangle))}{\int d\mathbf{p} \langle f(\mathbf{p}) \rangle}.$$

Use of the thermal momentum distribution yields $\langle f \rangle \approx 0.23$ and $S/A \approx 2.7$ for the $^{14}\text{N} + ^{27}\text{Al}$ reaction. For a distribution with nonequilibrium features, these values should represent the lower limit on the average occupation and the upper limit on the entropy. Indeed, for the source from the transport model and a thermal distribution, we find an entropy about 0.5 per nucleon higher than the entropy calculated directly within the model.

We have shown how to determine the relative source functions for particles directly from correlation data. When going beyond the Gaussian fitting, direct Fourier inversion, or simply fitting the source, the singular value decomposition [17] might be useful. This method allows one to determine what kind of source parametrization can be narrowed practically down by the correlation data.

ACKNOWLEDGMENTS

The authors thank Dariusz Miśkowiec and Peter Braun-Munzinger for providing them the pion correlation data in a numerical form. They further acknowledge the conversations with

colleagues, that have planted the seeds for this work, in particular with Herbert Ströbele, George Bertsch, and Scott Pratt. Finally, the authors thank Volker Koch for reading the manuscript. This work was partially supported by the National Science Foundation under Grant PHY-9403666 and by the Department of Energy under Grant FG06-90ER40561.

REFERENCES

- [1] J. T. Armstrong *et al.*, *Physics Today* 48, 42 (1995).
- [2] D. Buscher *et al.*, *Mon. Not. R. Astro. Soc.* 245, 7p (1990).
- [3] D. H. Boal, C. K. Gelbke, and B. K. Jennings, *Rev. Mod. Phys.* 62, 553 (1990).
- [4] G. F. Bertsch, *Phys. Rev. Lett.* 72, 2349 (1994).
- [5] S. Mrówczyński, *Phys. Lett. B* 277, 43 (1992).
- [6] S. Pratt, T. Csörgő, and J. Zimányi, *Phys. Rev. C* 42, 2646 (1990).
- [7] P. Danielewicz and P. Schuck, *Phys. Lett. B* 274, 268 (1992).
- [8] P. Danielewicz and D. Brown, in preparation.
- [9] G. Baym and P. Braun-Munzinger, report nucl-th/9606055, 1996.
- [10] D. Miśkowiec (E877 Collaboration), *Nucl. Phys. A* 610 (1996).
- [11] Y. D. Kim *et al.*, *Phys. Rev. Lett.* 67, 14 (1991).
- [12] W. G. Gong *et al.*, *Phys. Rev. C* 47, R429 (1993).
- [13] W. G. Gong *et al.*, *Phys. Rev. C* 43, 1804 (1991).
- [14] B. Kämpfer *et al.*, *Phys. Rev. C* 48, R955 (1993).
- [15] V. G. J. Stoks *et al.*, *Phys. Rev. C* 49, 2950 (1994).
- [16] P. Danielewicz, *Phys. Rev. C* 51, 716 (1995).
- [17] W. H. Press *et al.*, *Numerical Recipes* (Cambridge U. Press, Cambridge, 1986).

FIGURES

FIG. 1. Relative distribution of emission points for negative pion determined from the correlation data of Ref. [10]. Prior to the integration in Eq. (9), the relative momenta in the correlation function have been increased by 8% to correct for the Coulomb effect of the source; similar reduction of the momenta in the positive-pion correlation function brings the two correlation functions (or the source functions) into rough agreement with each other. The shaded area represents uncertainty in the source function associated with the uncertainty in the determination of the π^- correlation function [10] and due to the choice of $q_{\max} \approx 50$ MeV/c.

FIG. 2. Two-proton correlation function for the $^{14}\text{N} + ^{27}\text{Al}$ reaction at 75 MeV/nucleon. The symbols represent data [13,12] for three gates of total momentum imposed on protons emitted in the vicinity of $\theta_{\text{lab}} = 25^\circ$. The lines represent the correlation function for the extracted sources displayed in Fig. 3.

FIG. 3. Relative source function for protons emitted from the $^{14}\text{N} + ^{27}\text{Al}$ at 75 MeV/nucleon, in the vicinity of $\theta_{\text{lab}} = 25^\circ$, within three total momentum intervals. Filled circles represent the function extracted from the data [13,12]. Open circles represent the function determined within the Boltzmann-equation model [16].

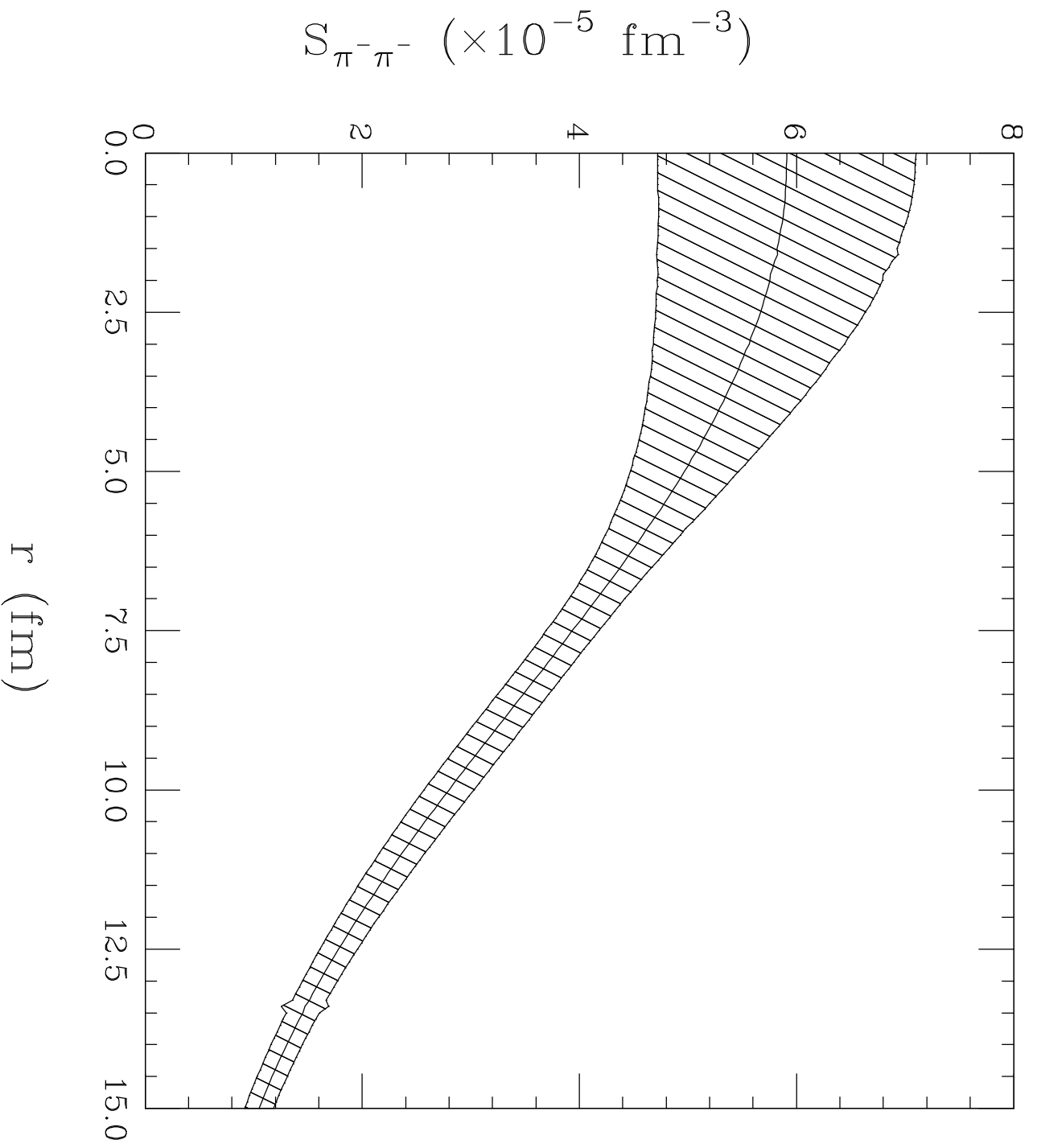


Figure 1

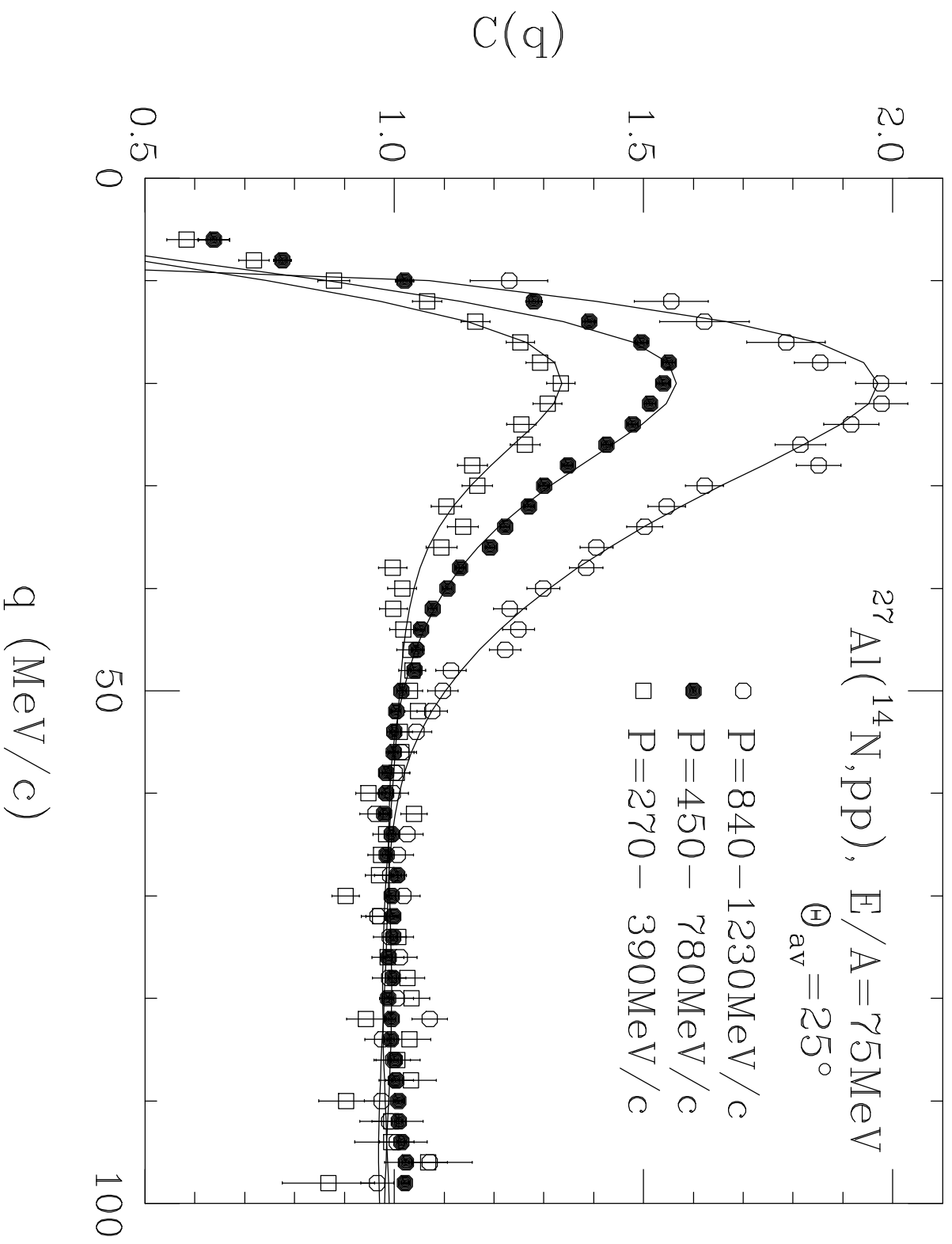


Figure 2

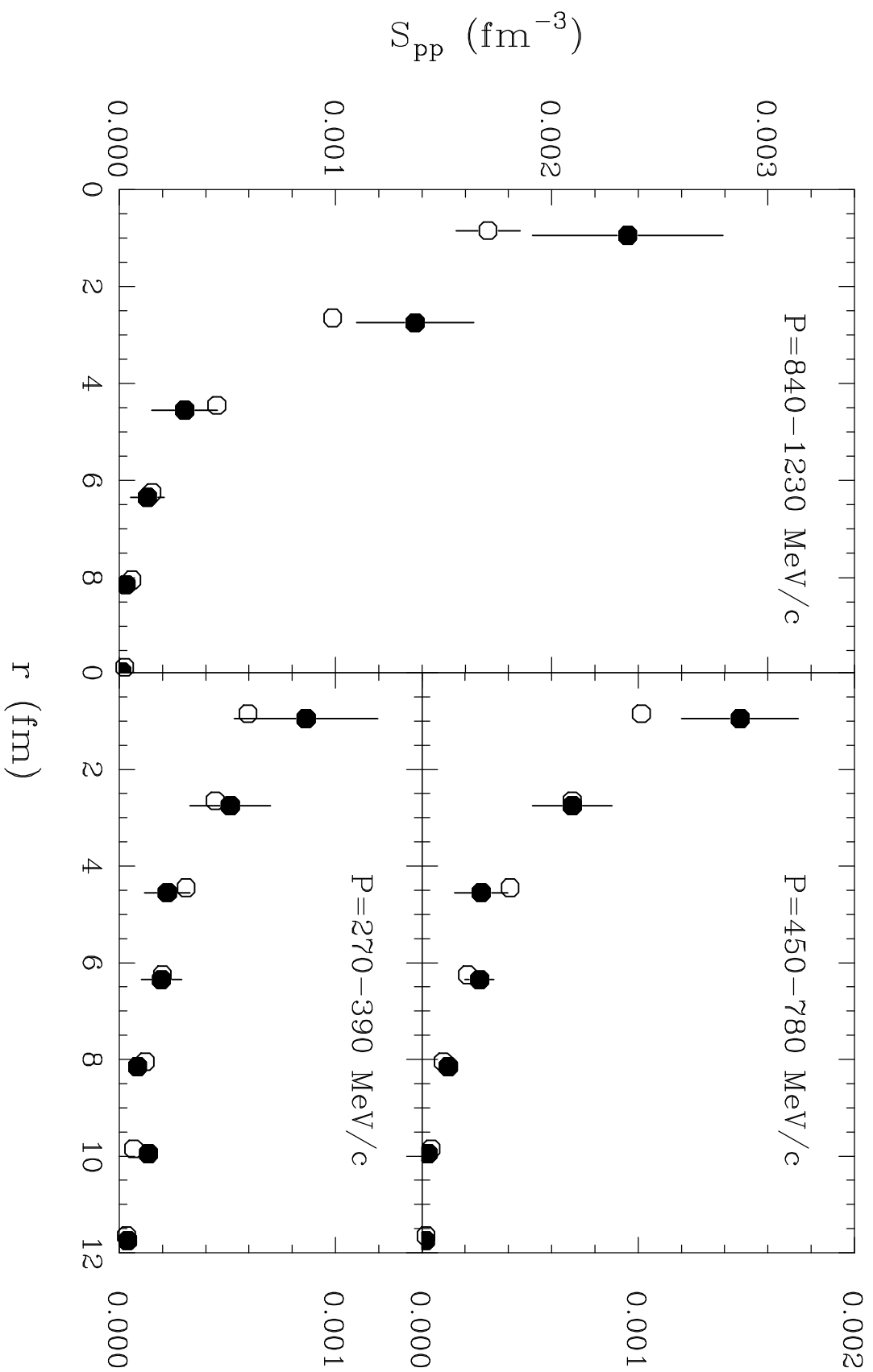


Figure 3